JOURNAL OF GENERAL VIROLOGY

RESEARCH ARTICLE

Poelaert *et al.*, *Journal of General Virology* 2019;100:1567–1579
DOI 10.1099/jgv.0.001317

MICROBIOLOGY SOCIETY

OPEN MICROBIOLOGY

Equine herpesvirus 1 infection orchestrates the expression of chemokines in equine respiratory epithelial cells

Katrien C. K. Poelaert[1], Jolien Van Cleemput[1,2], Kathlyn Laval[2], Jiexiong Xie[1], Herman W. Favoreel[1] and Hans J. Nauwynck[1,*]

Abstract

The ancestral equine herpesvirus 1 (EHV1), closely related to human herpes viruses, exploits leukocytes to reach its target organs, accordingly evading the immune surveillance system. Circulating EHV1 strains can be divided into abortigenic/neurovirulent, causing reproductive/neurological disorders. Neurovirulent EHV1 more efficiently recruits monocytic CD172a$^+$ cells to the upper respiratory tract (URT), while abortigenic EHV1 tempers monocyte migration. Whether similar results could be expected for T lymphocytes is not known. Therefore, we questioned whether differences in T cell recruitment could be associated with variations in cell tropism between both EHV1 phenotypes, and which viral proteins might be involved. The expression of CXCL9 and CXCL10 was evaluated in abortigenic/neurovirulent EHV1-inoculated primary respiratory epithelial cells (ERECs). The bioactivity of chemokines was tested with a functional migration assay. Replication of neurovirulent EHV1 in the URT resulted in an enhanced expression/bioactivity of CXCL9 and CXCL10, compared to abortigenic EHV1. Interestingly, deletion of glycoprotein 2 resulted in an increased recruitment of both monocytic CD172a$^+$ cells and T lymphocytes to the corresponding EREC supernatants. Our data reveal a novel function of EHV1-gp2, tempering leukocyte migration to the URT, further indicating a sophisticated virus-mediated orchestration of leukocyte recruitment to the URT.

INTRODUCTION

Chemokines are a large family of low-molecular-weight proteins that belong to the cytokine superfamily. They act through binding to their corresponding G protein-coupled receptors. It has become clear that specific chemokines and their receptors provide the molecular code responsible for the coordination of leukocyte trafficking [1, 2]. Together with their highly recognized roles in cell migration, these small proteins have multiple other functional properties, including cell survival and proliferation [3]. Their regulatory role in pathological and physiological perspectives result from hypersensitivity reactions, infections, angiogenesis, inflammation, tumour growth and haematopoietic development [2, 4–6]. Numerous studies have indicated that viruses that infect the respiratory tract, such as influenza virus, rhinovirus and herpes simplex virus 1 (HSV1), drive chemokine expression in the respiratory epithelium, resulting in the attraction of immune cells to the site of infection [7]. The upregulation of chemokine expression is mediated by two distinct mechanisms. First, pathogen-associated molecular pattern (PAMP) receptors at the mucosal surfaces recognize viral products such as HSV1 gH/gL and gB glycoproteins, viral RNA and CpG motifs, resulting in signal transduction through the ancestral PAMP recognition pathways [8, 9]. These signaling cascades induce the production of inflammatory chemokines either directly through nuclear factor kappa b (NF-κB) and mitogen-activated protein kinase (MAPK) activation and translocation to the nucleus, resulting in the transcription and translation of pro-inflammatory cytokines. Alternatively, inflammatory chemokines can become expressed indirectly through the expression of pro-inflammatory cytokines, such as type I IFN, TNFα, IL-1 and IL-6, which initiate the inflammatory response through the upregulation of NF-κB [10–13]. Secondly, antigen recognition by specific lymphocytes also drives chemokine expression, either directly or indirectly

Received 06 May 2019; Accepted 07 August 2019; Published 06 September 2019
Author affiliations: [1]Department of Virology, Immunology and Parasitology, Faculty of Veterinary Medicine, Ghent University, Salisburylaan 133, 9820 Merelbeke, Belgium; [2]Department of Molecular Biology 301 Schultz Laboratory, Princeton University Washington Rd, Princeton, NJ 08544, USA.
***Correspondence:** Hans J. Nauwynck, hans.nauwynck@ugent.be
Keywords: EHV1; chemokines; mononuclear cells; respiratory tract; glycoproteins.
Abbreviations: BFA, bredfeldin A; DPBS, Dulbecco's PBS; EHV1, equine herpesvirus 1; EREC, primary respiratory epithelial cell; FU, fluorescence unit; gG, glycoprotein G; gp2, glycoprotein 2; HSV1, herpes simplex virus 1; NK, natural killer; PAMP, pathogen-associated molecular pattern; PBMC, peripheral blood mononuclear cell; p.i., post-infection; ROI, region of interest; URT, upper respiratory tract; VZV, varicella zoster virus.
Supplementary material is available with the online version of this article.
001317 © 2019 The Authors
This is an open-access article distributed under the terms of the Creative Commons Attribution License, which permits unrestricted use, distribution, and reproduction in any medium, provided the original work is properly cited.

through the production of IFN and TNFα [14, 15]. Controlling herpes virus infections at the primary site of infection requires recruitment of immune cells, such as natural killer (NK) cells, T lymphocytes and monocytic cells [16, 17]. Those immune cells control viral replication through direct lysis of infected cells and cytokine production [18]. Type I IFN and CCL3 enhance NK cell recruitment to the site of infection [19, 20]. Monocytic cells are mainly recruited by monocyte chemoattractant protein-1 (MCP1 or CCL2) and, to a lesser extent, CCL5 (or RANTES) expressed by infected epithelial cells [18]. Multiple chemokines are described to attract T lymphocytes, including CXCL9 and CXCL10 [21].

Despite the protective antiviral effects of leukocytes, many viruses including several alphaherpes viruses are known to infect the cellular arm of the immune response as an immune evasive strategy to persist in their host. Equine herpes virus type 1 (EHV1), a virus closely related to the ubiquitous human HSV1 and varicella zoster virus (VZV), causes upper respiratory tract (URT) infections, abortion and neurological disease in horses worldwide [22, 23]. Respiratory problems occur upon primary viral replication in the epithelium of the URT. Although respiratory replication may have a subclinical outcome, clinical symptoms can include nasal discharge, fever and cough. EHV1 infects monocytic CD172a$^+$ cells and T lymphocytes and misuses these cells to cross the basement membrane and enter the blood circulation [24, 25]. During this cell-associated viraemia, EHV1 disseminates through the body and migrates to the secondary site of replication, the endothelium of the pregnant uterus or the central nervous system [22]. Abortions tend to occur after the seventh month of gestation [26]. Neurological disorders frequently present with hindlimb ataxia, atonia of the urine bladder and decreased tail tonus [27, 28]. Interestingly, EHV1 isolates circulating in the field can be differentiated as abortigenic, causing reproductive disorders, or neurovirulent variants, causing neurological disorders, based on a single nucleotide polymorphism in the gene that codes for DNA polymerase [29]. In the last 10 years, numerous researchers have reported unambiguous differences between both EHV1 phenotypes, essentially in the pathogen–host interactions [25, 30–35]. Vandekerckhove and colleagues [25] showed that neurovirulent variants infect three times more monocytic CD172a$^+$ cells earlier [24 h post-infection (p.i.)] in infection, compared to the abortigenic variants (36 h p.i.). At 24 h p.i., only neurovirulent strains were able to infect T lymphocytes. Later in infection (48-72 h p.i.), abortigenic variants infect four times more T lymphocytes compared to the neurovirulent variants. These findings were supported by the *ex vivo* study of Zhao *et al.* [33]. They showed that migration of monocytic CD172a$^+$ cells is controlled by upregulation of the expression of mainly chemo-attractant CCL2 at the primary site of infection. In addition, they demonstrated that primary replication of neurovirulent EHV1 variants attracted monocytic CD172a$^+$ cells more efficiently to the site of infection, resulting in a faster and more efficient infection of monocytic cells. Therefore, we hypothesized that neurovirulent variants might attract at an early stage also more T lymphocytes to the URT compared to abortigenic EHV1 strains, possibly by upregulating T lymphocyte-specific chemokines such as CXCL9 and CXCL10. Moreover, we questioned which viral proteins might influence the recruitment of mononuclear cells to the site of infection. Indeed, previous studies have demonstrated that the early glycoprotein G (gG) has chemokine binding activities. Interestingly, gG is conserved among different herpes viruses, including EHV1 [36]. von Einem *et al.* [37] showed that gG of EHV1 binds cellular chemokines and subsequently blocks their chemokine activity by preventing interaction with their corresponding receptors. Alongside gG, we hypothesized that other viral proteins might interact with the chemokine network in the URT. One putative candidate is the late viral glycoprotein 2 (gp2). This heavily *O*-glycosylated glycoprotein shows structural similarities with mucins, suggesting a similar mechanism of action. Interestingly, chemokine receptor (CCR) 5 in humans is heavily *O*-glycosylated in the chemokine-binding site at the N terminus, suggesting a putative role of the *O*-sulfated sugar moieties in the interaction with chemokines [38]. Additionally, deletion mutants of mucin-like glycoproteins of other viruses, such as paramyxoviruses, have been associated with elevated levels of cytokines, chemokines and type I IFN effects, resulting in a reduced viral replication in the URT [39–41]. In herpes viruses, alongside gp2 of EHV1, only HSV2 gG has been described to be heavily *O*-glycosylated [42].

In the present study, we used primary respiratory epithelial cells (ERECs) to visualize the expression of CXCL9 and CXCL10 upon infection with abortigenic and neurovirulent EHV1 variants. In addition, we analysed whether the produced chemokines are bioactive, and efficiently recruit mononuclear cells to the primary site of infection. Finally, we questioned which viral proteins might be involved in the viral interplay with immune modulatory chemokines. Understanding how EHV1 exploits chemokines to orchestrate its dissemination in the host is of key importance to develop new innovative antivirals and/or vaccination strategies.

METHODS

Virus

Different Belgian EHV1 isolates were included in this study and were genotyped in the ORF30 region by the Animal Health Trust in the UK. The EHV1 abortigenic strains 97P70, 438/77 and RacL11 were originally isolated from an aborted fetus, and encode an asparagine at amino acid position 752 (N_{752}) [43–45]. Strains 438/77 and the RacL11 lacking gG (438/77ΔgG) or gp2 (RacL11Δgp2) were constructed by Huang *et al* [46]. and Rudolph *et al.* [47], respectively. The neurovirulent 03P37 and 95P105 EHV1 strains were isolated in 2003 and 1995, respectively, from the blood of a paralytic horse [48], and encode aspartic acid at amino acid position 752 (D_{752}). The last passage of each strain was performed in RK-13 cells.

Donor horses

Respiratory tissues from horses were collected *post mortem* at the moment of slaughter, in the slaughterhouse. Horses negative for ocular/nasal discharge and lung pathologies were selected. The horses were aged between 5 and 15 years old, as determined by inspection of dental incisive architecture [49]. Each experiment was conducted with primary cells isolated from three different horses. The proximal part of the trachea was collected from each horse. Tissues were transported to the laboratory on ice, in PBS, supplemented with 1 % gentamycin, 1 % penicillin-streptomycin (Gibco), 1 % kanamycin (Sigma-Aldrich) and 0.5 % amphotericin B (Bristol-Myers Squibb).

Cells

Isolation and cultivation of primary respiratory epithelial cells

The isolation and cultivation of ERECs was conducted as previously described [32, 50]. Briefly, equine tracheal tissues were washed twice with cold Dulbecco's PBS (DPBS; Gibco) to remove red blood cells. Epithelial cells were isolated by an enzymatic digestion using gentle agitation in calcium- and magnesium-free minimal essential medium (MEM; Gibco) containing 1.4 % pronase (Roche Applied Science) and 0.1 % deoxyribonuclease I (Sigma-Aldrich). Tissues were incubated at 4 °C for 48 h with the enzyme mix. Cells were cultured in a plastic uncoated Petri dish for 6 h in DMEM/F12 (Gibco) containing calcium- and magnesium-free MEM, 1 % penicillin-streptomycin and 2.4 µg insulin ml^{-1} (Sigma-Aldrich) to reduce fibroblast contamination. ERECs were seeded at a concentration of 1.8×10^6 cells per well into type IV collagen- (Sigma-Aldrich) coated transwell cell culture wells of 0.4 µm pore size (Costar, Corning, Fisher Scientific) in DMEM/F12, containing 5 % non-heat-inactivated FBS (Gibco), 1 % calcium- and magnesium-free MEM, 1% penicillin-streptomycin and 0.5 % amphotericin B. After 24 h of culture, ERECs were cultivated at the air–liquid interface in epithelial cell medium containing DMEM/F12 supplemented with 2 % Ultroser G (Pall Life Sciences), 1 % penicillin-streptomycin and 0.5 % amphotericin B. ERECs were incubated in a 37 °C, 5 % CO_2, humidified incubator to confluency.

Isolation of monocytic CD172a$^+$ cells and T lymphocytes

Peripheral blood was sampled from the external vena jugularis into heparin (Leo) at a final concentration of 15 U ml^{-1}. The Ethical Committee of the Faculty of Veterinary Medicine, Ghent University (EC2017/118), approved the collection of blood. Fresh blood was diluted in an equal volume of DPBS without calcium and magnesium (Gibco). Peripheral blood mononuclear cells (PBMCs) were isolated as described by Poelaert *et al.* [35], by density centrifugation on Ficoll-Paque (d=1.077 g ml^{-1}) (GE Healthcare, Life Sciences) at 800 ***g*** for 30 min at 18 °C. The interphase band, containing the PBMCs, was collected and washed three times with DPBS. Cells were resuspended in complete medium based on Roswell Park Memorial Institute (RPMI) medium (Gibco), supplemented with 5 % newborn FCS (Gibco), 1 % MEM non-essential amino acids, 1 % sodium pyruvate, 1 % penicillin-streptomycin and 0.5% gentamycin (Gibco). PBMCs were then seeded at a concentration of 5×10^6 cells ml^{-1} in a plastic Petri dish and cultivated at 37 °C with 5 % CO_2. After 2 h, non-adhering leukocytes were removed by washing cells three times with RPMI medium and the adherent cells were cultured in complete medium. Non-adherent cells were washed three times with ice-cold RPMI. The cell pellet was incubated with 400 µl of mouse monoclonal (mAb) anti-horse pan B-cell, clone CVS36 (IgG1; 1:50) (Bio-Rad), diluted in ice-cold DPBS, for 1 h at 4 °C with gentle agitation. Cells were then washed once in magnetic-activated cell sorting (MACS) buffer containing DPBS supplemented with 1 mM EDTA and 5 % newborn FCS and incubated with 400 µl rat anti-mouse IgG microbeads (MACS Miltenyi Biotec) diluted in MACS buffer (1:5), for 1 h at 4 °C with gentle agitation. Next, the cells were washed once in MACS buffer and resuspended in 3 ml MACS buffer for application to the MACS column. The unbound cells of the pan-B-cell antibody-incubated T lymphocytes were collected from the column and consisted of >90 % of CD3$^+$ cells, assessed by flow cytometry after incubation with an mAb anti-CD3, clone UC-F6G (IgG1; 1:50) (UCDavis), directed against cells from the T cell lineage, followed by goat anti-mouse IgG FITC (1:200) (Molecular Probes). All T lymphocytes were cultured in basal medium [RPMI, 1 % MEM non-essential amino-acids, 1 % sodium pyruvate, 1 % BSA (Sigma-Aldrich) and antibiotics] supplemented with 4 U ml^{-1} recombinant interleukin-2 (hIL-2) (R&D systems) and 50 mM β-mercaptoethanol (β-ME) (Gibco). IL-2 is a prototypical T lymphocyte growth factor, which stimulates T cell survival and proliferation *in vitro* [51, 52]. After 6 h of cultivation, medium of the adherent monocytic cells was substituted by basal medium. The next day, CD172a$^+$ monocytic cells were detached from the plastic by incubation with Accumax solution (Sigma-Aldrich) for 30 min at 37 °C, 5 % CO_2. Monocytic cells and T lymphocytes were washed in ice-cold RPMI, centrifuged at 300 ***g*** and resuspended in basal medium.

EHV1 inoculation of primary respiratory epithelial cells (ERECs)

The basolateral inoculation of ERECs was executed as described by Van Cleemput *et al.* [53]. ERECs were (mock-) inoculated with 100 µl inoculum containing strains 97P70, 438/77, 438/77ΔgG, RacL11, RacL11Δgp2, 03P37 or 95P105 EHV1 at an m.o.i. of 0.1. After 45 min of incubation, non-absorbed virus particles were removed by washing the ERECs three times with DMEM/F12. Fresh EREC medium was added to the bottom plate wells and cells were further incubated at the air–liquid interface. At 24 h p.i., ERECs were fixed in methanol for 20 min at –20 °C, and stored at –20 °C until further processing.

Chemotaxis assay

Supernatants of mock- or EHV1-inoculated ERECs were collected at 24 h p.i. Chemotactic activity of the supernatants was determined using a 96-well Boyden chamber containing 5-µm pore size membranes (CytoSelect, Cell

Biolabs), following the manufacturer's guidelines. Briefly, supernatants of the mock- or EHV1-inoculated ERECs (150 µl) were applied to the wells of the feeder tray, before inserting the membrane tray. Medium containing 10 % FCS (Gibco) was included as a positive control. Equine CD172a$^+$ monocytic cells or T lymphocytes were resuspended in basal medium containing RPMI supplemented with antibiotics, at a concentration of 5×10^6 cells ml^{-1}, and 100 µl of each cell-type solution was added to the membrane tray. The chemotaxis chamber was transferred to 37 °C, 5 % CO_2 for 24 h, followed by dislodging the cells from the underside of the membrane in the harvesting tray. In a clean 96-well plate, 75 µl from the feeder tray and 75 µl from the harvesting tray were mixed with 50 µl of lysis buffer, containing CyQuant GR dye. Finally, 150 µl of the mixture, containing lysis buffer and dye, was transferred to a new 96-well plate, suitable for fluorescence measurement (Greiner). Cell migration was analysed by a Fluoroskan Ascent FL (ThermoFisher Scientific) plate reader. Cell migration values were measured at 480/520 nm, and were reported as fluorescence units (FU). The background FU-value was subtracted from the values of the supernatants of the mock-inoculated ERECs. FU-values of mock-inoculated ERECs were equalized as 1. Next, relative FU values were calculated as the percentage of the corresponding virus titre of the ERECs (FU-value/virus titre).

Indirect immunofluorescence staining

Protocol

At 24 h p.i., ERECs were pre-treated with brefeldin A (BFA; Sigma-Aldrich) at 10 µg ml^{-1} for 45 min prior to fixation. EHV1 proteins were stained with biotinylated equine polyclonal anti-EHV1 IgG antibody (1:20 in DPBS) [48], followed by streptavidin TR (1:200 in DPBS) (Molecular Probes). CXCL9 and CXCL10 were visualized by incubating with a rabbit polyclonal anti-CXCL9 antibody (IgG; GeneTex) (1:50 in DPBS) or a rabbit polyclonal anti-CXCL10 antibody (IgG; Kingfisher Biotech) (1:50 in DPBS) followed by an FITC-conjugated goat anti-rabbit IgG antibody (1:100 in DPBS) (Molecular Probes). In parallel, ERECs were incubated with irrelevant isotype controls (1:50 in DPBS). All antibodies were incubated for 1 h at 37 °C. All antibodies were diluted in DPBS. Cell nuclei were counterstained with Hoechst 33342 (10 µg ml^{-1}) (Molecular Probes).

Analysis of expression of CXCL9 and CXCL10

Five viral plaques per condition per horse were analysed. The intensity of chemokine expression in the respiratory epithelium was measured using ImageJ software (US National Institutes of Health). The region of interest (ROI, i.e. viral plaques) was drawn manually for each picture in the 'ROI manager tool'. Next, the threshold value to distinguish between regions with or without chemokine expression was determined, and the percentage of chemokine-positive area was calculated.

Confocal microscopy

Immunofluorescence of cryosections and ERECs was analysed by confocal microscopy (Leica TCS SP2 Laser Scanning Spectral Confocal System; Leica Microsystems). A Gre-Ne 543 nm laser was used to excite Texas Red fluorochromes. An Ar 488 nm laser excited FITC fluorochromes.

Prediction of *O*-glycosylation sites

The predicted *O*-glycosylation sites of the amino acid sequence of gene 70 (encoding gG) and gene 71 (encoding gp 2) of abortigenic and neurovirulent EHV1 strains were obtained through NetOglyc@cbs.dtu.dk, using the algorithm of Hansen *et al.* [54], as previously described by Wellington *et al.* [55].

Three-dimensional model viral glycoproteins

The predictive three-dimensional model of gG and gp2 were obtained through I-Tasser (http://zhanglab.ccmb.med.umich.edu), and was analysed with the Pymol Protein Viewer.

Statistical analyses

We analysed the data for statistical significance via a multiple-way ANOVA. If the assumption of equal variables was not fulfilled with Levene's test, the data were log-transformed prior to ANOVA. If the normality of the residuals was not achieved after log-transformation, a Kruskal–Wallis test followed by a Mann–Whitney post-hoc test was performed. Differences in results with P-values <0.05 were considered statistically significant. The data shown represent the means+SD of independent experiments. Data were statistically evaluated with IBM SPSS Statistics for Windows, version 24.0 (IBM).

RESULTS

CXCL9 and CXCL10 are upregulated during EHV1 replication in ERECs

At 12 or 24 h p.i., ERECs were treated with 10 µg BFA ml^{-1} to prevent chemokine secretion from the cell and to optimize CXCL9 and CXCL10 visualization by immunofluorescence staining. The expression of CXCL9 could be observed at 12 h p.i. (data not shown) and visibly co-localized with viral plaques of both EHV1 variants at 24 h p.i. for all EHV1 strains (Fig. 1a). EHV1-inoculated ERECs detached at 36 h p.i., which prevented staining of chemokines at later time points. Therefore, all subsequent experiments were conducted at 24 h p.i. At 24 h p.i., the intensity of CXCL9 expression was slightly higher in epithelial cells inoculated with the neurovirulent 03P37 and 95P105 strains compared to that of cells inoculated with the abortigenic 438/77 strain (P=0.055 and P=0.141, respectively). No significant difference was observed between both neurovirulent strains and the abortigenic 97P70 (P>0.05). The expression pattern of CXCL10 clearly differed from that of CXCL9. In the area of a viral plaque, only single cells were CXCL10-positive, and no differences were observed between EHV1 variants (P>0.05). Positive cells were not observed in the non-inoculated areas of the epithelium (Fig. 1b). Together, we demonstrated that the replication of both EHV1 variants activates the chemokine response to a greater (CXCL9) or lesser (CXCL10) extent in the respiratory epithelium. The expression of CXCL9 was more apparent

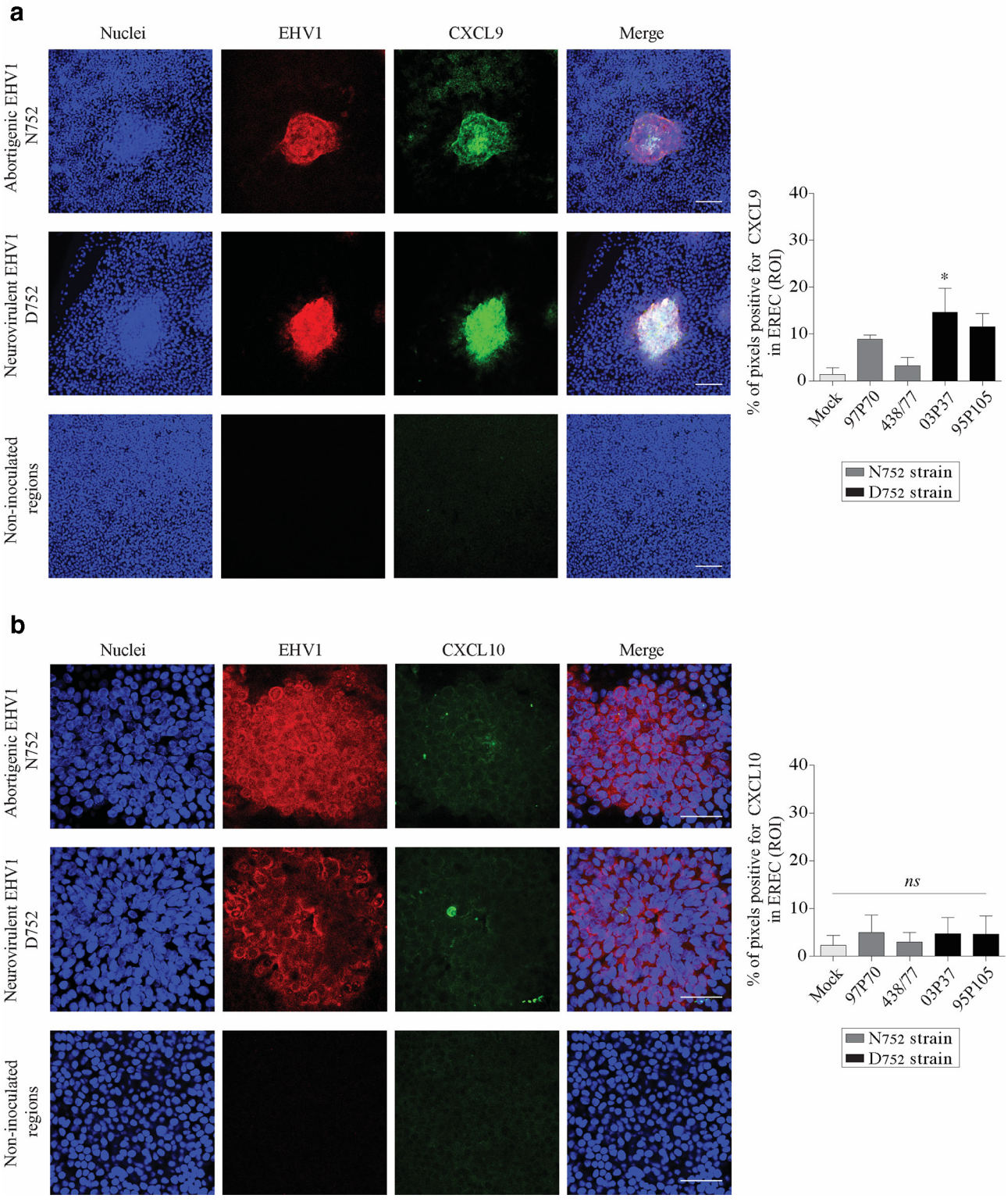

Fig. 1. Expression patterns of CXCL9 and CXCL10 in mock-, abortigenic (N752) EHV1, or neurovirulent (D752) EHV1-inoculated ERECs. The left panel shows representative confocal images of the immunofluorescence staining, with (a) CXCL9 or (b) CXCL10 stained in green (FITC), viral proteins stained in red (TR), and nuclei counterstained in blue (Hoechst) in mock- or EHV1-inoculated ERECs, at 24 h p.i. Bars, 75 µm. The right panel shows the intensity of CXCL9 or CXCL10 signal in the ERECs at the level randomly chosen for viral plaques. Data are represented as means+SD, and *ns* indicates no statistically significant differences. *Statistically significant differences at $P<0.05$. Experiments were performed with ERECs isolated from three individual horses.

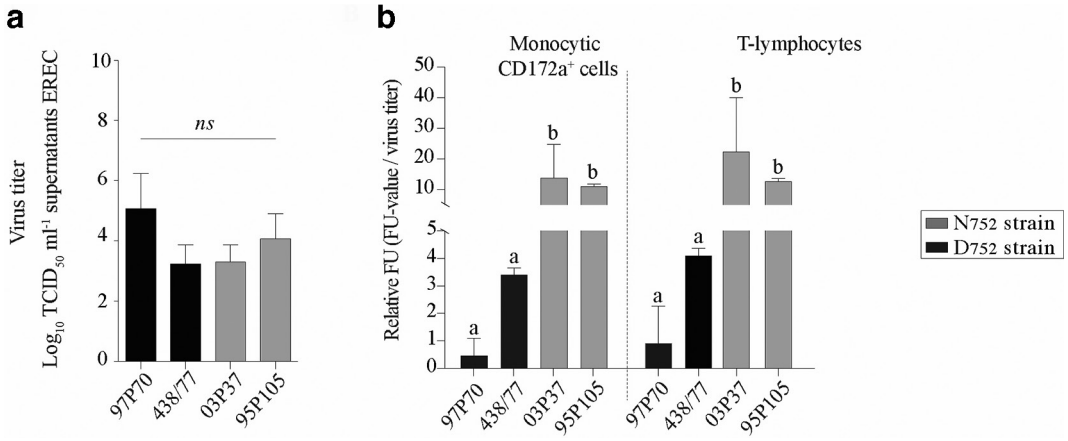

Fig. 2. Abortigenic (N752) and neurovirulent (D752) EHV1 replication in ERECs induce the production of bioactive chemokines. (a) Virus titre of the abortigenic (97P70 and 438/77) and neurovirulent (03P37 and 95P105) EHV1-inoculated ERECs. (b) Chemotactic activities of the supernatants of the abortigenic (97P70 and 438/77) or neurovirulent (03P37 and 95P105) EHV1-inoculated ERECs were tested in a cell recruitment assay. Results are shown as a percentage of the corresponding virus titre. Data are shown as means+SD, different letters indicate statistically significant differences, and *ns* indicates not statistically significant differences. Experiments were performed with supernatants of ERECs derived from three individual horses.

upon infection with the neurovirulent variant, compared to the abortigenic variant. In contrast, CXCL10 was expressed only by single cells in viral plaques of both viral strains.

Replication of EHV1 in ERECs induces the recruitment of mononuclear cells to the site of infection

Zhao *et al.* [33] indicated the upregulation of CCL2 in the respiratory mucosa upon infection with the neurovirulent EHV1 variant. This was less efficient upon inoculation with EHV1 strains of the abortigenic phenotype. These results were confirmed in the current EREC model, as shown in Fig. S1 (available with the online version of this article). Thus, replication of neurovirulent and, to a lesser extent, abortigenic EHV1 in respiratory epithelial cells induces chemokine secretion. To determine whether these chemokines are biologically active and recruit monocytic CD172a$^+$ cells and T lymphocytes to the site of infection, a functional migration assay was performed. First, we analysed the replication of both variants in ERECs. No significant differences in extracellular virus titre were observed between the included EHV1 strains (P=0.111) (Fig. 2a). Next, we measured the chemotactic activity of the supernatants of mock- or EHV1-inoculated ERECs in a cell migration assay. As viral replication induces the production of chemokines, data are shown as a relative FU-value normalized to the corresponding virus titre. Supernatants of both abortigenic and neurovirulent EHV1-inoculated ERECs attracted monocytic CD172a$^+$ cells and T lymphocytes (Fig. 2b). However, supernatants derived from ERECs inoculated with the neurovirulent 03P37 or 95P105 EHV1 strains attracted more monocytic CD172a$^+$ cells (13.8±10.9 or 12.7±1, respectively), compared to that of the abortigenic 97P70 (0.5±0.6) (P<0.05) or 438/77 EHV1 strains (4.1±0.3) (P<0.05). In addition, the neurovirulent 03P37 and 95P105 strains recruited significantly more T lymphocytes (22.3±17.8 and 13.0±1.0), compared to the supernatant derived from 97P70 (0.9±1.3) (P<0.05) and 438/77 (4.1±0.3) (P<0.05) EHV1-inoculated ERECs. Together, we observed differences in the chemotactic capacities of the supernatants of ERECs inoculated with EHV1 strains belonging to the different phenotypes. We found that the replication of neurovirulent 03P37 and 95P105 strains in the *in vitro* EREC-model attracted more monocytic CD172a$^+$ and T cells compared to the included abortigenic 97P70 and 438/77 EHV1 strain.

Early gG and late gp2 temper the recruitment of mononuclear cells to the URT

gG of several alphaherpes viruses, including EHV1, is known as a chemokine-binding protein [36, 56–58]. It binds to chemokines with high affinity and inhibits their biological activity by preventing their interaction with specific cell receptors [56]. First, we evaluated the replication kinetics of EHV1-ΔgG in ERECs. The number of plaques induced by EHV1-ΔgG was not significantly different compared to the parental EHV1 strain (P>0.05) (Fig. 3a, left panel). The latitude of the 438/77ΔgG-induced viral plaques was slightly larger compared to the parental strain (P=0.109) (Fig. 3a, middle panel). The extracellular virus titre measured in the supernatant of 438/77ΔgG inoculated ERECs (1±1 $\log_{10}$ $TCID_{50}$ ml^{-1}) was slightly but not significantly lower than the virus titre of the parental 438/77 (4.0±4.0 $\log_{10}$ $TCID_{50}$ ml^{-1}) (P=0.272) (Fig. 3a, right panel). Because the replication kinetics of parental and mutant EHV1 strains differ, we standardized the FU-values based on the corresponding virus titres. Deletion of gG resulted in a 91±51-fold increase in the migration of monocytic CD172a$^+$ cells (P<0.05), and a 86±61-fold increased migration of T lymphocytes (P<0.05), compared to the parental strain (Fig. 3B).

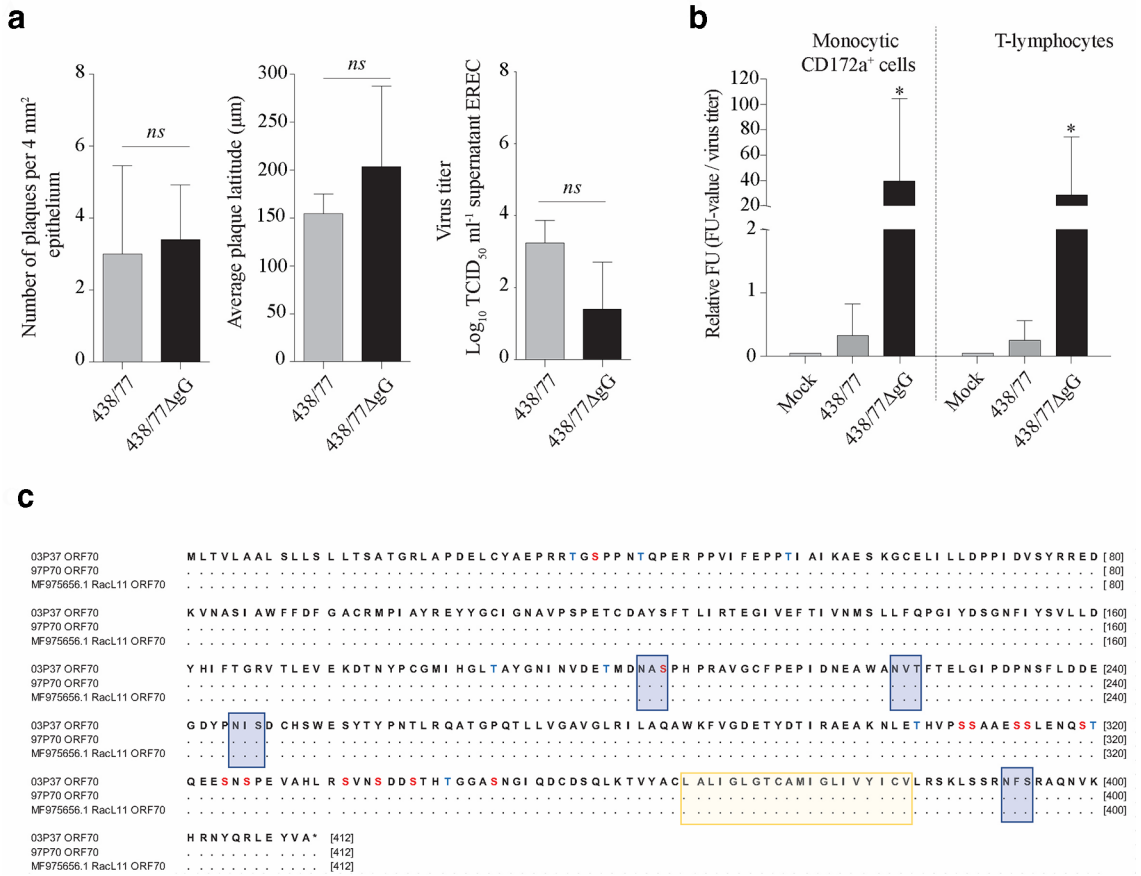

Fig. 3. gG impedes the recruitment of mononuclear cells to the EHV1-infected respiratory epithelium. (a) Replication kinetics of the gG-deletion mutant, and their corresponding parental strain in ERECs. (b) Recruitment of monocytic CD172a⁺ cells and T lymphocytes to the supernatants of the ERECs, inoculated with the gG-deletion mutant and their parental strain, shown as the relative FU-value as a percentage of the corresponding virus titre. (c) Alignment of gG (pORF70) amino acid sequences of neurovirulent 03P37 and abortigenic 97P70 and RacL11 EHV1 strains. Dots represent residues that are identical, and hyphens indicate gaps. Blank dotted boxes indicate regions with variations between the indicated EHV1 strains. Blue boxes indicate predicted *N*-glycosylation sites. Red or blue labelled letters indicate predicted *O*-glycosylated serine or threonine, respectively, residues with a prediction strength of more than 0.5. The yellow box indicates the transmembrane region.

In order to determine whether variations in EHV1-gG might be associated with the different chemokine activity of both EHV1 phenotypes, the amino acid sequence of the abortigenic and neurovirulent EHV1 strains were compared. No apparent variations at the level of amino acid sequence or in glycosylation were observed, suggesting no alteration between abortigenic and neurovirulent EHV1 variants (Fig. 3c). Lacking the availability of a full sequence of 438/77, we were not able to include the amino acid sequence of gG of the abortigenic 438/77 strain.

In parallel, we analysed the role of the mucin-like late gp2 in the orchestration of leukocyte migration to the URT. First, we evaluated the replication kinetics of the EHV1 gp2-deletion mutant in ERECs by analysing the number and latitude of viral plaques, and virus titration. The number of RacL11Δgp2 viral plaques was significantly lower compared with the parental strain (P<0.05) (Fig. 4a, left panel). No differences in plaque latitudes (Fig. 4a, middle panel) or virus titre (Fig. 4a, right panel) of EHV1-Δgp2 and the parental strain were observed in ERECs (P>0.05). Deletion of gp2 led to an 8±6-fold (P<0.05) and 24±9-fold (P<0.05) increase in the recruitment of monocytic CD172a⁺ cells and T lymphocytes, respectively, compared to the parental virus (Fig. 4a). Remarkably, indirect immunofluorescence staining of ERECs inoculated with RacL11Δgp2 did not show any alterations in the CXCL9 chemokine expression compared to their corresponding parental strain (Fig. 4c and d). A careful analysis of the amino acid sequence of the 03P37 neurovirulent EHV1 strain, and different abortigenic EHV1 strains, indicated alterations in the amino acid sequence of gp2 (Fig. 5a). We included 97P70, RacL11 (GenBank accession number MF975656.1) and 438/77 (GenBank accession number AY034645.1) abortigenic EHV1 strains and 03P37 neurovirulent EHV1 strain. Because the full genome sequence of 95P105 is not available, we were not able to include this strain in the sequence analysis. Multiple variations were observed at amino acid position 196 until

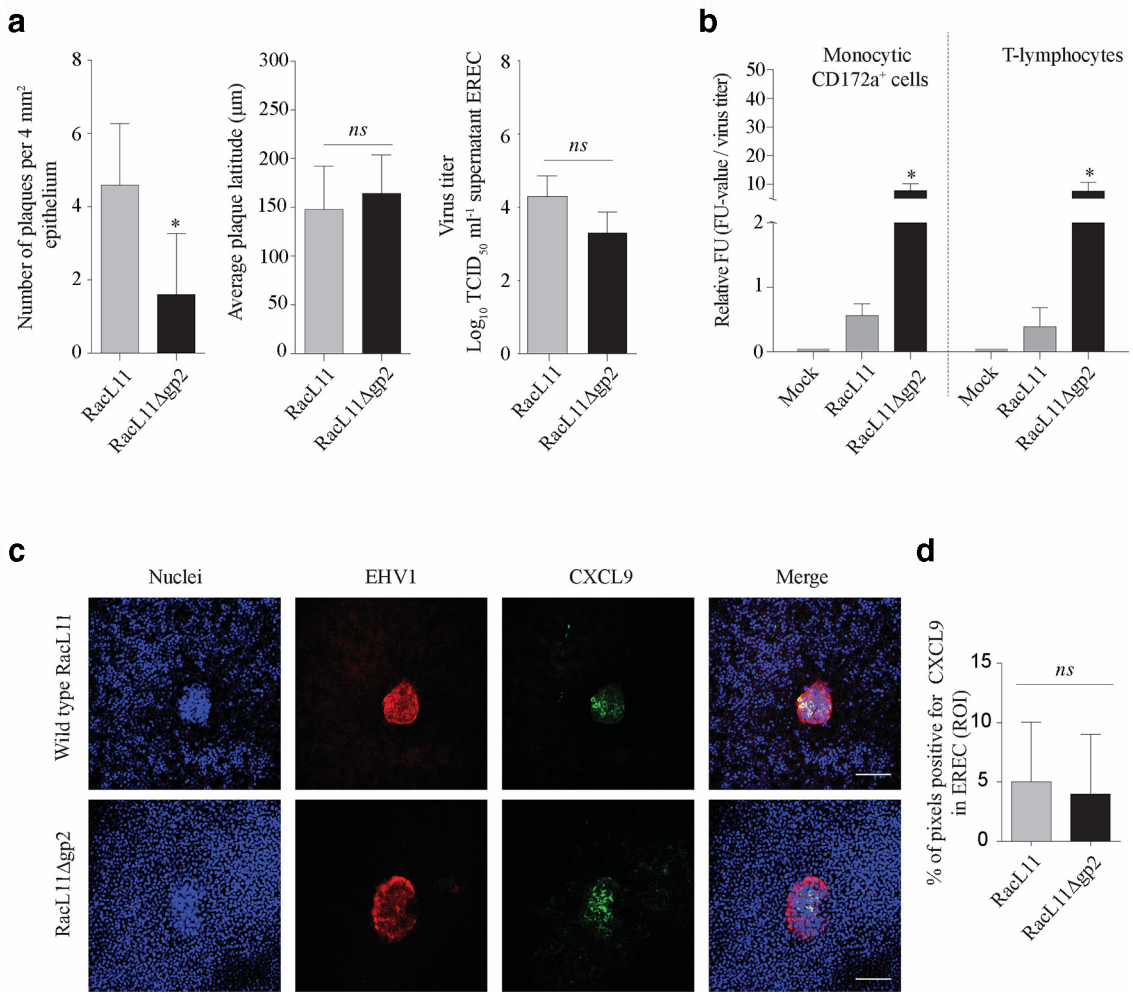

Fig. 4. gp2 impedes the recruitment of mononuclear cells to the EHV1-infected respiratory epithelium. (a) Replication kinetics of the gp2-deletion mutant, and their corresponding parental strain in ERECs. (b) Recruitment of monocytic CD172a⁺ cells and T lymphocytes to the supernatants of the ERECs, inoculated with the gp2-deletion mutant and their parental strain, shown as the relative FU-value as a percentage of the correspondent virus titre. (c) Representative confocal images of CXCL9 (FITC) expression in RacL11- or RacL11Δgp2-infected ERECs viral proteins were stained with (TR). Nuclei were counterstained in blue (Hoechst). Bars, 75 µm. (d) The intensity of CXCL9 signal in the ERECs at the level randomly chosen for viral plaques. Data are represented as means+SD and *ns* indicates no statistical difference. *Statistically significant differences at $P<0.05$. Experiments were performed with supernatants of ERECs derived from three individual horses.

position 253. We mainly observed substitutions between the polar, hydrophilic amino acids serine (S) or threonine (T), and the aliphatic, hydrophobic alanine (A). The latter amino acid alterations resulted in an extra β-sheet in the gp2 structure of the abortigenic variant (Fig. 5b). In addition, variations at the protein level resulted in variations in glycosylation. Indeed, at amino acid positions 601, 629 and 630 we observed variations in *O*-glycosylation between the included EHV1 strains. The neurovirulent 03P37 EHV1 strain and abortigenic RacL11 strain were both *O*-glycosylated at all three positions, while the 97P70 abortigenic EHV1 strain was not. The abortigenic 438/77 EHV1 strain was only *O*-glycosylated at positions 601 and 629. This sequence analysis of different EHV1 strains might explain the alterations in recruitment of immune cells to the site of infection.

Taken together, we confirmed that EHV1-gG impedes the recruitment of monocytic CD172a⁺ cells and T lymphocytes to the epithelium of the URT. Alongside the early protein gG, we demonstrated that the late viral protein gp2 and possibly other late viral protein(s) interfere with chemokine activity, which may hinder the recruitment of both monocytic CD172a⁺ cells and T lymphocytes to the EHV1-infected respiratory epithelium.

DISCUSSION

Chemokines are essential at the mucosal barriers to guide (innate) immune effector cells to the site of tissue damage and pathogen replication [18]. Numerous reports have indicated the importance of leukocytes in clearing herpes virus

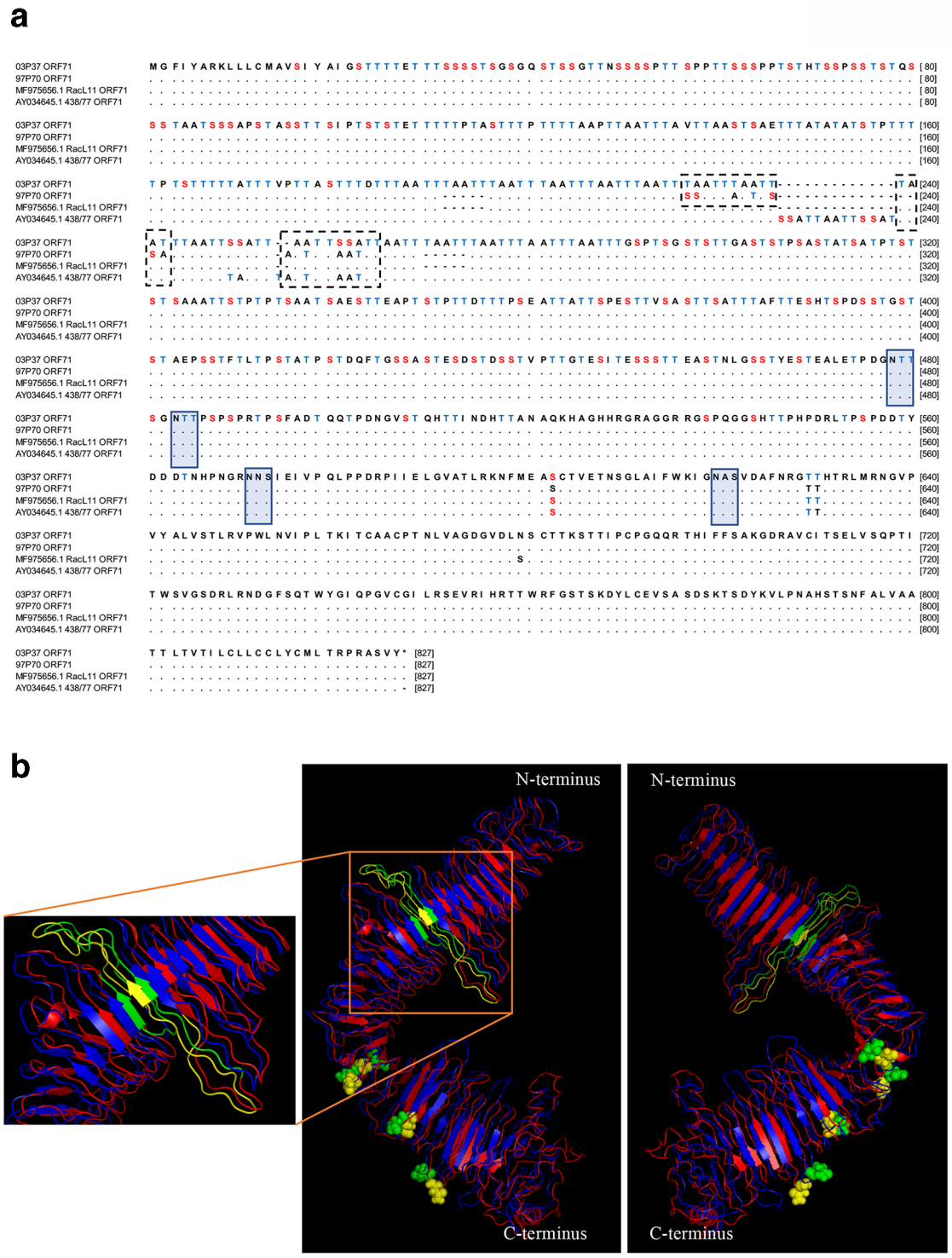

Fig. 5. Comparison of gp2 of abortigenic and neurovirulent EHV1 strains. (a) Alignment of gp2 (pORF71) amino acid sequences of neurovirulent 03P37 and abortigenic 97P70, RacL11 and 438/77 EHV1 strains. Dots represent residues that are identical, and hyphens indicate gaps. Blank dotted boxes indicate regions with variations between the indicated EHV1 strains. Blue boxes indicate predicted *N*-glycosylation sites. Red or blue labelled letters indicate predicted *O*-glycosylated serine or threonine, respectively, residues with a prediction strength of more than 0.5. (b) Comparison of predicted three-dimensional model of the abortigenic gp2 (red) and neurovirulent gp2 (blue). Yellow and green lines show the region of alterations between the neurovirulent and the abortigenic gp2, respectively. Yellow and green sugar structures indicate *N*-glycosylation sites of gp2 of the neurovirulent and abortigenic EHV1 strain, respectively. Arrowheads indicate variation in sugar positions.

infections. Indeed, $CD8^+$ T lymphocytes are essential in the elimination of viruses at mucosal barriers. Infection of cells involved in the immune response may represent one of the strategies to overcome viral elimination. Similar to HSV1 and VZV, EHV1 has developed a tropism for monocytic $CD172a^+$ cells and lymphocytes, as one of its multiple immune evasion strategies [59, 60]. Previous studies have indicated that neurovirulent EHV1 variants are more efficient in attracting and infecting monocytic $CD172a^+$ cells and T lymphocytes early in infection, compared to abortigenic variants. Abortigenic variants are more effective in infecting T lymphocytes later in infection, compared to the neurovirulent variants [24, 25, 33–35].

Numerous chemokines are associated with the attraction of T cells. CXCL9 and CXCL10 are inflammatory chemokines that specifically target T lymphocytes through the CXCR3 receptor. They are best known for their effects on activated $CD4^+$ Th1 cells, $CD8^+$ T cells and NK cells [61]. First, we questioned whether abortigenic and neurovirulent EHV1 replication activates the production of CXCL9 and CXCL10 in the URT. Using immunofluorescence staining, we observed that both EHV1 variants induce CXCL9 and CXCL10 expression in ERECs. The expression of CXCL9 clearly co-localized with EHV1-induced plaques, whereas CXCL10 was only expressed by single cells within a viral plaque. These results are in line with other herpes viruses, such as HSV1 and HSV2, indicating virus-induced expression of CXCL9 in (primary) human epithelial cells [62, 63]. We observed a propensity of enhanced CXCL9 production upon infection of ERECs with neurovirulent EHV1 strains, compared to the abortigenic strains. To examine whether the produced chemokines are biologically active, we included a functional cell migration assay. Replication of both EHV1 variants in ERECs led to the production of bioactive chemokines, which efficiently attracted mononuclear cells to the site of infection. In the EREC model we observed a trend of differences in the recruitment of mononuclear cells to the site of infection between the two EHV1 phenotypes. These results are in line with the *ex vivo* study by Zhao *et al.* [33]. They demonstrated an enhanced expression of monocytic chemoattractant CCL2 upon infection of the nasal mucosa with the neurovirulent variant by immunofluorescence staining. Here, we confirm that the produced chemokines are biologically active. Lacking specific equine neutralizing antibodies against chemokines limited the full characterization of the functional chemokines. Therefore, more research is needed to link the immunofluorescence staining with the functional cell migration assay. Our results confirm the previous results of the *ex vivo* study of Vandekerckhove *et al.* [25]. They reported that a neurovirulent EHV1 variant infects more monocytic $CD172a^+$ cells and T lymphocytes earlier (24 h p.i.) in infection, compared to an abortigenic EHV1 variant (36 h p.i.).

Combining the results of the CXCL9/10 immunofluorescence staining with the functional cell migration assay, we propose that neurovirulent EHV1 strains stimulate the release of chemokines, resulting in massive recruitment and subsequently direct infection of monocytic $CD172a^+$ cells and T cells in the URT. In contrast, the abortigenic EHV1 strains appear to temper and regulate the recruitment of immune cells to the primary site of replication during the first 36 h p.i., to avoid viral elimination. Next, the abortigenic EHV1 strains mainly target monocytic $CD172a^+$ cells early in infection. Once T cells are recruited to the URT, we suggest that infected monocytic $CD172a^+$ cells transfer infection to $CD4^+$ T cells. Indeed, we previously demonstrated that infected monocytic cells efficiently transfer infection to T lymphocytes [35]. More research is needed to further verify this hypothesis.

One of the best-studied viral chemokine scavengers is the early gG [36, 56–58]. Homologues of gG are conserved among alphaherpes viruses, including EHV1 and EHV4 [36]. gG of EHV1 binds to chemokines with high affinity and blocks chemokine activity by preventing interaction with their specific receptors [36, 58]. Here, we confirm the interaction of EHV1-gG with the chemokine network of the EHV1-infected ERECs. Deletion of gG resulted in increased chemotaxis of the main target cells of EHV1, monocytic $CD172a^+$ cells and T lymphocytes. This is in line with the *in vitro* study of Viejo-Borbolla et al. [64], demonstrating that PrV-gG and EHV1-gG bind to specific chemokines, including CCL2, CCL5 and CXCL9, resulting in a reduced number of migrated cells. However, the latter results could not be associated with the observed differences between abortigenic or neurovirulent variants. Indeed, sequence analysis of gG of the abortigenic EHV1 strains and neurovirulent 03P37 EHV1 strain did not show any difference in nucleotide or amino acid sequence. Based on the several differences in the immune evasion strategy of the abortigenic and neurovirulent EHV1 phenotype [24, 25, 30–33], we hypothesized that both variants possibly not only differ in ORF30 [29, 65], but also in other (non-)structural viral proteins. Although gG is expressed with early viral gene kinetics, blocking the transcription of late viral proteins of the abortigenic variant resulted in increased recruitment of mononuclear cells to supernatants of infected ERECs, indicating that additional, late viral proteins may also be involved (data not shown). Intriguingly, Whittaker *et al.* [42] reported similarities in glycosylation, and lectin-binding capacities between EHV1 gp2 and HSV2 gG. First, we inoculated ERECs with EHV1-Δgp2 and analysed the replication kinetics. Interestingly, we found a significant reduction in the number of viral plaques in ERECs when gp2 was deleted, compared to the parental strain. These results are in line with the *in vitro* study of Rudolph and Osterrieder [47]. This is not surprising given that gp2 is heavily *O*-glycosylated. Iversen and colleagues [66] demonstrated that *O*-linked sugars of HSV2 are essential for optimal viral entry. Virus pretreatment with specific enzymes to remove *O*-linked sugar moieties from the EHV1 surface would be an interesting first analysis to specify the role of *O*-linked sugars during EHV1 entry in ERECs. In addition, those specific sugar moieties on gp2 could have considerable effects on the protein conformation as well as protein assembly, stability and function [67, 68]. It is important to note that all results concerning gp2 in this paper are based on the abortigenic RacL11 strain. However, based on our results, we hypothesized that gp2 of EHV1 might

have similar chemokine-binding activities as gG. Indeed, we found that deletion of the unique gp2 resulted in an increased chemotaxis of mainly T lymphocytes, and to a lesser extent monocytic CD172a$^+$ cells, compared to the parental strain. These results are in line with the *in vivo* study of Wimer *et al.* [69]. They demonstrated *in vivo* that the occurrence of fever is delayed/accelerated depending on the presence/absence of gp2 in the viral strain. However, they could not correlate gp2 with increased infection of mononuclear cells and thus increased viraemia. Therefore, more research is required to elucidate the specific role of gp2 in the recruitment of mononuclear cells to the site of infection for both EHV1 variants.

In conclusion, we have demonstrated that the *in vitro* culture of ERECs represents an efficient model to analyse virus-induced upregulation and bioactivity of chemokines. Replication of the EHV1 neurovirulent strain and to a lesser extent abortigenic EHV1 strain enhances the expression of specific chemokines in the URT. We showed that EHV1 replication in ERECs induces the production of biologically active chemokines, such as CXCL9 and CXCL10, which efficiently attract mononuclear cells. Moreover, we showed an enhanced recruitment of monocytic CD172a$^+$ cells and T lymphocytes upon infection with neurovirulent 03P37 and 95P105 EHV1 compared with the abortigenic 97P70 and 438/77 EHV1 strain. We confirmed that gG of EHV1 plays a crucial role in the chemotaxis of mononuclear target cells to the primary site of replication. Alongside the early viral protein gG, we demonstrated that gp2 impedes the recruitment of mononuclear cells in the *in vitro* EREC model.

Funding information
This research was funded by 'Institute for the promotion of Innovation through Science and Technology in Flanders' (IWT-Vlaanderen) (141627). K.P. was funded by the Institute for the promotion of Innovation through Science and Technology in Flanders (IWT-Vlaanderen) (141627). J.V.C. was funded by the Research Foundation Flanders (FWO) (11Y5415N). This research was supported by grants from the Special Research Fund of Ghent University (G.O.A. grant 01G01317).

Acknowledgements
The authors acknowledge Professor Dr M. Studdert (Australia) for providing the 438/77 gG deletion mutant, and Prof. Dr N. Osterrieder (Germany) for providing the RacL11 gp2 deletion mutant. The authors are grateful to Carine Boone, Nele Dennequin, Chantal Vanmaercke, and Jonathan Vandenbogaerde for their excellent technical support.

Author contributions
Conceptualization, K.P., J.V.C., H.N.; methodology, K.P., J.V.C., K.L., H.N.; validation, K.P.; formal analysis, K.P.; investigation, K.P.; resources, K.P., H.N.; data curation, K.P.; writing-original draft preparation, K.P.; writing-review and editing, K.L., H.F., H.N.; visualization, K.P., J.X.; supervision, H.F., H.N.; project administration, H.N.; funding, H.F., H.N.

Conflicts of interest
The authors declare that there are no conflicts of interest.

References

1. Griffith JW, Sokol CL, Luster AD. Chemokines and chemokine receptors: positioning cells for host defense and immunity. *Annu Rev Immunol* 2014;32:659–702.
2. Stone M, Hayward J, Huang C, E. Huma Z, Sanchez J. Mechanisms of regulation of the chemokine-receptor network. *Int J Mol Sci* 2017;18:342.
3. Reinhart TA, Qin S, Sui Y. Multiple roles for chemokines in the pathogenesis of SIV infection. *Curr HIV Res* 2009;7:73–82.
4. Nibbs RJB, Graham GJ. Immune regulation by atypical chemokine receptors. *Nat Rev Immunol* 2013;13:815–829.
5. Abendroth A, Morrow G, Cunningham AL, Slobedman B. Varicella-Zoster virus infection of human dendritic cells and transmission to T cells: implications for virus dissemination in the host. *J Virol* 2001;75:6183–6192.
6. Suresh P, Wanchu A. Chemokines and chemokine receptors in HIV infection: role in pathogenesis and therapeutics. *J Postgrad Med* 2006;52:210–217.
7. Schaller M, Hogaboam CM, Lukacs N, Kunkel SL. Respiratory viral infections drive chemokine expression and exacerbate the asthmatic response. *J Allergy Clin Immunol* 2006;118:295–302.
8. Leoni V, Gianni T, Salvioli S, Campadelli-Fiume G. Herpes simplex virus glycoproteins gH/gL and gB bind Toll-like receptor 2, and soluble gH/gL is sufficient to activate NF-κB. *J Virol* 2012;86:6555–6562.
9. Paludan SR, Bowie AG, Horan KA, Fitzgerald KA. Recognition of herpesviruses by the innate immune system. *Nat Rev Immunol* 2011;11:143–154.
10. Bonnet MC, Weil R, Dam E, Hovanessian AG, Meurs EF. Pkr stimulates NF-kappaB irrespective of its kinase function by interacting with the IkappaB kinase complex. *Mol Cell Biol* 2000;20:4532–4542.
11. Zamanian-Daryoush M, Mogensen TH, DiDonato JA, Williams BR. Nf-Kappab activation by double-stranded-RNA-activated protein kinase (PKR) is mediated through NF-kappaB-inducing kinase and IkappaB kinase. *Mol Cell Biol* 2000;20:1278–1290.
12. Gil J, García MA, Gomez-Puertas P, Guerra S, Rullas J *et al*. Traf family proteins link PKR with NF-kappa B activation. *Mol Cell Biol* 2004;24:4502–4512.
13. Kawai T, Akira S. Innate immune recognition of viral infection. *Nat Immunol* 2006;7:131–137.
14. Huse M, Lillemeier BF, Kuhns MS, Chen DS, Davis MM. T cells use two directionally distinct pathways for cytokine secretion. *Nat Immunol* 2006;7:247–255.
15. Olson TS, Ley K. Chemokines and chemokine receptors in leukocyte trafficking. *Am J Physiol Regul Integr Comp Physiol* 2002;283:R7–R28.
16. Bukowski JF, Welsh RM. The role of natural killer cells and interferon in resistance to acute infection of mice with herpes simplex virus type 1. *Journal of immunology* 1986;136:3481–3485.
17. Thompson MR, Kaminski JJ, Kurt-Jones EA, Fitzgerald KA. Pattern recognition receptors and the innate immune response to viral infection. *Viruses* 2011;3:920–940.
18. Sokol CL, Luster AD. The chemokine system in innate immunity. *Cold Spring Harb Perspect Biol* 2015;7:a016303.
19. Biron CA, Nguyen KB, Pien GC, Cousens LP, Salazar-Mather TP. Natural killer cells in antiviral defense: function and regulation by innate cytokines. *Annu Rev Immunol* 1999;17:189–220.
20. Trinchieri G. Biology of natural killer cells. *Adv Immunol* 1989;47:187–376.
21. Mackay CR. Chemokines: immunology's high impact factors. *Nat Immunol* 2001;2:95–101.
22. Edington N, Bridges CG, Patel JR. Endothelial cell infection and thrombosis in paralysis caused by equid herpesvirus-1: equine stroke. *Arch Virol* 1986;90:111–124.
23. Crabb BS, Studdert MJ. Equine herpesviruses 4 (equine rhinopneumonitis virus) and 1 (equine abortion virus). *Adv Virus Res* 1995;45:153–190.
24. Gryspeerdt AC, Vandekerckhove AP, Garré B, Barbé F, Van de Walle GR *et al*. Differences in replication kinetics and cell tropism between neurovirulent and non-neurovirulent EHV1 strains during the acute phase of infection in horses. *Vet Microbiol* 2010;142:242–253.

25. Vandekerckhove AP, Glorieux S, Gryspeerdt AC, Steukers L, Duchateau L *et al*. Replication kinetics of neurovirulent versus non-neurovirulent equine herpesvirus type 1 strains in equine nasal mucosal explants. *J Gen Virol* 2010;91:2019–2028.
26. Bryans JT, Allen GP. Herpesviral Diseases of the Horse. In: Wittmann G (editors). *Herpesvirus Diseases of Cattle, Horses, and Pigs*. Boston, MA: Springer US; 1989. pp. 176–229.
27. Goehring LS, van Winden SC, van Maanen C, Sloet van Oldruitenborgh-Oosterbaan MM. Equine herpesvirus type 1-associated myeloencephalopathy in the Netherlands: a four-year retrospective study (1999-2003). *J Vet Intern Med* 2006;20:601–607.
28. Goehring LS, Hussey GS, Ashton LV, Schenkel AR, Lunn DP. Infection of central nervous system endothelial cells by cell-associated EHV-1. *Vet Microbiol* 2011;148:389–395.
29. Nugent J, Birch-Machin I, Smith KC, Mumford JA, Swann Z *et al*. Analysis of equid herpesvirus 1 strain variation reveals a point mutation of the DNA polymerase strongly associated with neuropathogenic versus nonneuropathogenic disease outbreaks. *J Virol* 2006;80:4047–4060.
30. Laval K, Favoreel HW, Nauwynck HJ. Equine herpesvirus type 1 replication is delayed in CD172a+ monocytic cells and controlled by histone deacetylases. *J Gen Virol* 2015;96:118–130.
31. Laval K, Van Cleemput J, Poelaert KC, Brown IK, Nauwynck HJ. Replication of neurovirulent equine herpesvirus type 1 (EHV-1) in CD172a^{+} monocytic cells. *Comp Immunol Microbiol Infect Dis* 2017;50:58–62.
32. Poelaert KCK, Van Cleemput J, Laval K, Favoreel HW, Soboll Hussey G *et al*. Abortigenic but not neurotropic equine herpes virus 1 modulates the interferon antiviral defense. *Front Cell Infect Microbiol* 2018;8:312.
33. Zhao J, Poelaert KCK, Van Cleemput J, Nauwynck HJ. Ccl2 and CCL5 driven attraction of CD172a+ monocytic cells during an equine herpesvirus type 1 (EHV-1) infection in equine nasal mucosa and the impact of two migration inhibitors, rosiglitazone (RSG) and quinacrine (Qc). *Vet Res* 2017;48.
34. Holz CL, Nelli RK, Wilson ME, Zarski LM, Azab W *et al*. Viral genes and cellular markers associated with neurological complications during herpesvirus infections. *J Gen Virol* 2017;98:1439–1454.
35. Poelaert KCK, Van Cleemput J, Laval K, Favoreel HW, Couck L *et al*. Equine herpesvirus 1 Bridles T lymphocytes to reach its target organs. *J Virol* 2019;93:JVI.02098–18.
36. Drummer HE, Studdert MJ, Crabb BS. Equine herpesvirus-4 glycoprotein G is secreted as a disulphide-linked homodimer and is present as two homodimeric species in the virion. *J Gen Virol* 1998;79:1205–1213.
37. von Einem J, Smith PM, Van de Walle GR, O'Callaghan DJ, Osterrieder N. In vitro and in vivo characterization of equine herpesvirus type 1 (EHV-1) mutants devoid of the viral chemokine-binding glycoprotein G (gG). *Virology* 2007;362:151–162.
38. Bannert N, Craig S, Farzan M, Sogah D, Santo NV *et al*. Sialylated O-glycans and sulfated tyrosines in the NH2-terminal domain of CC chemokine receptor 5 contribute to high affinity binding of chemokines. *J Exp Med* 2001;194:1661–1674.
39. Biacchesi S, Skiadopoulos MH, Yang L, Lamirande EW, Tran KC *et al*. Recombinant human metapneumovirus lacking the small hydrophobic SH and/or attachment G glycoprotein: deletion of G yields a promising vaccine candidate. *J Virol* 2004;78:12877–12887.
40. Biacchesi S, Pham QN, Skiadopoulos MH, Murphy BR, Collins PL *et al*. Infection of nonhuman primates with recombinant human metapneumovirus lacking the SH, G, or M2-2 protein categorizes each as a nonessential accessory protein and identifies vaccine candidates. *J Virol* 2005;79:12608–12613.
41. Bao X, Liu T, Shan Y, Li K, Garofalo RP *et al*. Human metapneumovirus glycoprotein G inhibits innate immune responses. *PLoS Pathog* 2008;4:e1000077.
42. Whittaker GR, Wheldon LA, Giles LE, Stocks JM, Halliburton IW *et al*. Characterization of the high Mr glycoprotein (gP300) of equine herpesvirus type 1 as a novel glycoprotein with extensive O-linked carbohydrate. *J Gen Virol* 1990;71:2407–2416.
43. van Der Meulen KM, Nauwynck HJ, Buddaert W, Pensaert MB. Replication of equine herpesvirus type 1 in freshly isolated equine peripheral blood mononuclear cells and changes in susceptibility following mitogen stimulation. *J Gen Virol* 2000;81:21–25.
44. Studdert MJ, Simpson T, Roizman B. Differentiation of respiratory and abortigenic isolates of equine herpesvirus 1 by restriction endonucleases. *Science* 1981;214:562–564.
45. Mayr A, Pette J, Petzoldt K, Wagener K. Untersuchungen Zur Entwicklung eines Lebendimpfstoffes gegen die rhinopneumonitis (Stutenabort) Der Pferde1). *Zentralblatt für Veterinärmedizin Reihe B* 1968;15:406–418.
46. Huang J, Hartley CA, Ficorilli NP, Crabb BS, Studdert MJ. Glycoprotein G deletion mutants of equine herpesvirus 1 (EHV1; equine abortion virus) and EHV4 (equine rhinopneumonitis virus). *Arch Virol* 2005;150:2583–2592.
47. Rudolph J, Osterrieder N. Equine herpesvirus type 1 devoid of gM and GP2 is severely impaired in virus egress but not direct cell-to-cell spread. *Virology* 2002;293:356–367.
48. van der Meulen K, Vercauteren G, Nauwynck H, Pensaert M. A local epidemic of equine herpesvirus 1-induced neurological disorders in Belgium. *Vlaams Diergeneeskundig Tijdschrift* 2003;72:366–372.
49. Muylle S, Simoens P, Lauwers H. Ageing horses by an examination of their incisor teeth: an (im)possible task? *Vet Rec* 1996;138:295–301.
50. Quintana AM, Landolt GA, Annis KM, Hussey GS. Immunological characterization of the equine airway epithelium and of a primary equine airway epithelial cell culture model. *Vet Immunol Immunopathol* 2011;140:226–236.
51. Verbsky JW, Chatila TA. Chapter 23 - Immune Dysregulation Leading to Chronic Autoimmunity. Sullivan KE and Stiehm ER (editors). Stiehm's Immune Deficiencies. Amsterdam: Academic Press; 2014. pp. 497–516.
52. Geginat J, Sallusto F, Lanzavecchia A. Cytokine-driven proliferation and differentiation of human naive, central memory, and effector memory CD4$^{(+)}$ T cells. *J Exp Med* 2001;194:1711–1720.
53. Van Cleemput J, Poelaert KCK, Laval K, Maes R, Hussey GS *et al*. Access to a main alphaherpesvirus receptor, located basolaterally in the respiratory epithelium, is masked by intercellular junctions. *Sci Rep* 2017;7:16656.
54. Hansen JE, Lund O, Engelbrecht J, Bohr H, Nielsen JO *et al*. Prediction of O-glycosylation of mammalian proteins: specificity patterns of UDP-GalNAc:polypeptide *N*-acetylgalactosaminyltransferase. *Biochem J* 1995;308:801–813.
55. Wellington JE, Allen GP, Gooley AA, Love DN, Packer NH *et al*. The highly O-glycosylated glycoprotein GP2 of equine herpesvirus 1 is encoded by gene 71. *J Virol* 1996;70:8195–8198.
56. Bryant NA, Davis-Poynter N, Vanderplasschen A, Alcami A. Glycoprotein G isoforms from some alphaherpesviruses function as broad-spectrum chemokine binding proteins. *Embo J* 2003;22:833–846.
57. Colle CF, O'Callaghan DJ. Transcriptional analyses of the unique short segment of EHV-1 strain Kentucky a. *Virus Genes* 1995;9:257–268.
58. Thormann N, Van de Walle GR, Azab W, Osterrieder N. The role of secreted glycoprotein G of equine herpesvirus type 1 and type 4 (EHV-1 and EHV-4) in immune modulation and virulence. *Virus Res* 2012;169:203–211.
59. Aubert M, Yoon M, Sloan DD, Spear PG, Jerome KR. The virological synapse facilitates herpes simplex virus entry into T cells. *J Virol* 2009;83:6171–6183.
60. Schaap A, Fortin J-F, Sommer M, Zerboni L, Stamatis S *et al*. T-Cell tropism and the role of ORF66 protein in pathogenesis of varicella-zoster virus infection. *J Virol* 2005;79:12921–12933.
61. Müller M, Carter S, Hofer MJ, Campbell IL. Review: The chemokine receptor CXCR3 and its ligands CXCL9, CXCL10 and CXCL11 in

neuroimmunity--a tale of conflict and conundrum. *Neuropathol Appl Neurobiol* 2010;36:368–387.

62. Huang W, Hu K, Luo S, Zhang M, Li C *et al*. Herpes simplex virus type 2 infection of human epithelial cells induces CXCL9 expression and $CD4^+$ T cell migration via activation of p38-CCAAT/enhancer-binding protein-β pathway. *J Immunol* 2012;188:6247–6257.
63. Molesworth-Kenyon SJ, Milam A, Rockette A, Troupe A, Oakes JE *et al*. Expression, inducers and cellular sources of the chemokine Mig (CXCL 9), during primary herpes simplex virus type-1 infection of the cornea. *Curr Eye Res* 2015;40:800–808.
64. Viejo-Borbolla A, Muñoz A, Tabarés E, Alcamí A. Glycoprotein G from pseudorabies virus binds to chemokines with high affinity and inhibits their function. *J Gen Virol* 2010;91:23–31.
65. Goodman LB, Loregian A, Perkins GA, Nugent J, Buckles EL *et al*. A point mutation in a herpesvirus polymerase determines neuropathogenicity. *PLoS Pathog* 2007;3:e160.
66. Iversen MB, Reinert LS, Thomsen MK, Bagdonaite I, Nandakumar R *et al*. An innate antiviral pathway acting before interferons at epithelial surfaces. *Nat Immunol* 2016;17:150–158.
67. Kobata A. Structures and functions of the sugar chains of glycoproteins. *European Journal of Biochemistry* 1992;209:483–501.
68. Hart GW, Kreppel LK, Comer FI, Arnold CS, Snow DM *et al*. O-Glcnacylation of key nuclear and cytoskeletal proteins: reciprocity with O-phosphorylation and putative roles in protein multimerization. *Glycobiology* 1996;6:711–716.
69. Wimer CL, Damiani A, Osterrieder N, Wagner B. Equine herpesvirus type-1 modulates CCL2, CCL3, CCL5, CXCL9, and CXCL10 chemokine expression. *Vet Immunol Immunopathol* 2011;140:266–274.

Five reasons to publish your next article with a Microbiology Society journal

1. The Microbiology Society is a not-for-profit organization.
2. We offer fast and rigorous peer review – average time to first decision is 4–6 weeks.
3. Our journals have a global readership with subscriptions held in research institutions around the world.
4. 80% of our authors rate our submission process as 'excellent' or 'very good'.
5. Your article will be published on an interactive journal platform with advanced metrics.

Find out more and submit your article at microbiologyresearch.org.